

Full paper



# A ZnO micro/nanowire-based photonic synapse with piezo-phototronic modulation

Guofeng Hu<sup>a</sup>, Hua An<sup>a</sup>, Jianguo Xi<sup>b</sup>, Junfeng Lu<sup>d</sup>, Qilin Hua<sup>b,c,\*</sup>, Zhengchun Peng<sup>a,\*\*</sup>

<sup>a</sup> Key Laboratory of Optoelectronic Devices and Systems of Ministry of Education and Guangdong Province, College of Physics and Optoelectronic Engineering, Shenzhen University, Shenzhen 518060, China

<sup>b</sup> CAS Center for Excellence in Nanoscience, Beijing Key Laboratory of Micro-nano Energy and Sensor, Beijing Institute of Nanoenergy and Nanosystems, Chinese Academy of Sciences, Beijing 101400, China

<sup>c</sup> School of Nanoscience and Technology, University of Chinese Academy of Sciences, Beijing 100049, China

<sup>d</sup> College of Science, Nanjing University of Aeronautics and Astronautics, Nanjing 211106, China

## ARTICLE INFO

### Keywords:

Photonic synapse  
Piezo-phototronic effect  
ZnO micro/nanowire  
Neuromorphic computing

## ABSTRACT

Neuromorphic computing systems that emulate the working principle of the biological brain is capable of overcoming the von Neumann bottleneck. Artificial synapses are critical information processing units in the neuromorphic computing systems. Because of the fast speed, large bandwidth, and high reliability, light or photonic interaction controlled artificial synapses (i.e., photonic synapses) are receiving great attention in recent years. Applying an additional stimuli to the photonic synapse will lead to a multi-level adjustment of synaptic plasticity behavior, which is useful for developing a multi-sensory neuromorphic system. In this work, we present a transparent and flexible photonic synapse based on a single ZnO micro/nanowire with modulation by piezo-phototronic effect, which is coupling by strain-induced piezoelectric effect and photoexcitation. The synaptic functions including paired-pulse facilitation, short-term plasticity, and long-term plasticity are demonstrated with pulsed UV illumination. Furthermore, the synaptic weight change can be effectively modulated by applying compressive strains due to the piezo-phototronic effect induced in the ZnO micro/nanowire. Specifically, the weight change can be reduced from 1437.5% to 191.4% with a compressive strain change from  $-0.00\%$  to  $-0.28\%$  under a UV light pulse of  $4.2 \text{ mW cm}^{-2}$ . A mechanism is proposed to explain the observed phenomenon of the photonic synapse under compressive strains. In addition, the relaxation of long-term plasticity can be modulated by controlling the transport of photo-generated carriers through the Schottky contact via the piezo-phototronic effect. This work demonstrates an effective approach to developing photonic synapses with tunable functions for multi-sensory neuromorphic computing systems.

## 1. Introduction

With the rapid development of artificial intelligence, big data, and the Internet of Things, the von Neumann architecture-based computing systems, consisting of separate processor and memory units, are encountering fundamental physical limitations, such as energy consumption, access speed, and bandwidth [1–5]. On the contrary, the emerging neuromorphic computing architectures, which emulate the functionalities, effectiveness, capacity, and energy-efficiency of human brain, can overcome such limitations. The biological synapse in human brain is a critical unit for information processing, with both computing

and memory functions. In the meantime, synaptic plasticity characteristics, such as short-term plasticity (STP) and long-term plasticity (LTP), help the brain to efficiently process information in high-speed, fault-tolerance, and massive-parallel manners. Equivalently, artificial synapses emulating the biological synaptic behaviors have been developed with two-terminal memristors and three-terminal transistors modulated by electrical and/or light stimuli [6–9]. Recently, electronic synapses are having been intensively reported with emerging devices. However, such synapses typically exhibit limited operation speed, which is caused by the bandwidth-connection-density trade-off [10,11].

Impressively, photonic synapses can be a more favorable artificial

\* Corresponding author at: CAS Center for Excellence in Nanoscience, Beijing Key Laboratory of Micro-nano Energy and Sensor, Beijing Institute of Nanoenergy and Nanosystems, Chinese Academy of Sciences, Beijing 101400, China.

\*\* Corresponding author.

E-mail addresses: [huaqilin@binn.cas.cn](mailto:huaqilin@binn.cas.cn) (Q. Hua), [zcpeng@szu.edu.cn](mailto:zcpeng@szu.edu.cn) (Z. Peng).

<https://doi.org/10.1016/j.nanoen.2021.106282>

Received 13 May 2021; Received in revised form 14 June 2021; Accepted 21 June 2021

Available online 25 June 2021

2211-2855/© 2021 Published by Elsevier Ltd.

synapses due to their fast speed, large bandwidth, negligible crosstalk, and low-power consumption [7,9,12]. However, the photonic synapses reported so far have limited controllability on the synaptic behaviors such as relaxation properties of persistent photoconductivity. To overcome this problem, researchers have tried various methods including modulating the composition of materials, applying a gate voltage, and introducing a ferroelectric layer [13–15]. However, these methods increase the complexity of the device structure and the fabrication processes. Therefore, simple but effective alternative methods such as introducing the piezo-phototronic effect to modulate the photonic synaptic functions are becoming the hot spot of this field [16].

Piezoelectric semiconductor, usually existing in wurtzite/zinc blend family materials, e.g., ZnO, GaN, and ZnS, simultaneously possesses semiconducting and piezoelectric properties [17–21]. Owing to the non-central symmetric crystal structure, piezoelectric polarization charges can be created inside the semiconductor by applying a strain. The piezo-phototronic effect is to use this inner piezopotential as a “gate” voltage to tune the charge generation, separation, transport and/or recombination in optoelectronic processes. This effect has been widely utilized to modulate the performance of various piezotronic devices, such as photodetectors [22,23], solar cells [24,25], and LEDs [26,27]. More impressively, one-dimensional ZnO nanostructures, including nanowires and nanobelts, have important application prospects in strain-tunable electronics/optoelectronics, self-powered adaptive sensors, optical microelectromechanical systems, touchable haptic technologies and human-machine interfacing [22,28–31].

Here, we propose an effective way to modulate the synaptic plasticity of a single ZnO micro/nanowire (MNW)-based photonic synapse under the piezo-phototronic effect. The synaptic functions, such as paired-pulse facilitation (PPF), short-term plasticity (STP), and long-term plasticity (LTP), are explored using 365 nm ultraviolet (UV) pulses. More importantly, we demonstrate the ZnO MNW with a single crystalline structure is essential to serve as a model system to bring in the piezo-phototronic effect. Taking the advantage of this effect, we also investigate the regulation of the synaptic weight change by controlling the transport of photo-generated carriers in the ZnO MNW. This method not only provides an effective synaptic behavior modulation for the nanowire-based photonic synapses and strain-tunable electronics/optoelectronics, but also shows potential applications in strain sensing for biomedical sciences, bio-realistic artificial intelligence systems, neuro-morphic computing system and construction of next-generation neuro-morphic sensory network.

## 2. Experimental sections

### 2.1. ZnO MNWs synthesis and characterization

ZnO MNWs were fabricated by using a chemical vapor deposition (CVD) method [32,33]. ZnO and carbon mixed powders were placed in a quartz boat in the center of the tube furnace, while the silicon substrate coated with 5 nm Au was placed at downstream. The typical synthesis of ZnO MNWs was carried out at a temperature of 960 °C for 1 h with the Ar carrier gas flow rate of 100 sccm.

### 2.2. Device fabrication

The photonic synapse was fabricated by transferring an individual ZnO MNW laterally onto a flexible polystyrene (PS) substrate under a stereoscopic microscope, with its *c*-axis in the plane of the substrate pointing to the source. Then silver paste was applied to fix the two ends of the ZnO MNW at the substrate to form the source/drain electrodes.

### 2.3. Measurements of the photonic synapse

All measurements were carried out in ambient conditions at room temperature. The device was tightly fixed on a customized sample

holder by one end. At the same time, the other end of the device through moving a positioner which was attached to a 3D mechanical stage (Newport M-462) with a displacement resolution of 1 μm. The compressive strain was introduced by bending the other end of the device via moving the positioner. The light pulse stimuli were generated with a 365 nm UV lamp, and the intensities were adjusted by using a set of filters during the experiment. A function generator (Tektronix AFG3011C) was applied to the UV lamp. The customized set-up for measurements was used in our experiment as mentioned earlier [24]. The electrical and photoelectric properties of the photonic synapse under different strains were measured by a computer-controlled measurement system (Stanford research systems SR570 and DS345) under UV illumination.

## 3. Results and discussion

The photonic synapses have drawn great attention for faithfully emulating the functions of biological synapses in the rapid development of artificial intelligence techniques. Synaptic plasticity has played a crucial role in information storage and learning for synaptic functions. In this work, we introduced an effective method, the piezo-phototronic effect, to modulate synaptic plasticity in the photonic synapse based on a single ZnO MNW, and the conception diagram is shown in Fig. 1a. Firstly, as a semiconductor with a 3.37 eV of direct bandgap, ZnO exhibits excellent photo-response characteristics for the photonic synapse in the UV region. Secondly, the strain-induced piezo-potential generated in the ZnO could effectively modulate the interface charge carrier transport characteristics to optimize the performance of the device [18–21]. Thus, for ZnO with unique semiconducting, photoexciting, and piezoelectric properties simultaneously, the coupling among them has formed the novel physical effect of piezo-phototronics. Under this mechanism, the behavior of photonic synapse could be effectively modulated.

ZnO MNWs were grown by using a mixed powder of zinc oxide and graphite via vapor-liquid-solid method at 960 °C. Fig. 1b shows a typical scanning electron microscopy (SEM) image of the as-grown ZnO MNWs. Their length could reach several hundred micrometers, and their diameters varies from hundreds of nanometers to several micrometers. An enlarged SEM image of an individual ZnO NW is shown as an inset in Fig. 1b to reveal the hexagonal cross-section with a smooth surface (around 6.5 μm in diameter). The growth direction of ZnO MNWs was determined along the +*c*-axis as mentioned earlier [24]. The UV-vis absorption and photoluminescence (PL) spectra are presented in Fig. 1c, which exhibited an absorption edge of 378 nm (corresponding to 3.28 eV), and a strong near-band-edge emission (NBE) peak at about 390.8 nm. A broad peak clearly observed around 540 nm was attributed to the oxygen-related defects, such as  $V_{\text{O}}^0$  and  $V_{\text{O}}^+$ , which are important for affecting electrical and photoelectric properties of ZnO [34]. An optical micrograph and an image of the as-fabricated device were shown in Fig. 1d and e, respectively. The transparent and flexible device is demonstrated and suitable to apply dynamic strains under UV illumination.

In a brain, the synapse is the connection between two neurons, which transmits information from pre-to post-neuron through electrical or electrochemical signals, as shown in Fig. 2a. The influx and extrusion of  $\text{Ca}^{2+}$  in the pre- and post-neuron play an important role in modulating the synaptic plasticity [14,15]. The synaptic weight, or strength of the connection, could change in response to the input stimuli from the pre-neuron. That is, the synapse is critical for information processing. To emulate the biological synapse, a simple two-terminal flexible photonic synapse is fabricated by using a single ZnO MNW. The increases of conductance for carrier generation triggered by light pulse and decay of conductance under dim ambience for photonic synapse resemble the influx and extrusion dynamics of  $\text{Ca}^{2+}$  in the biological synapse. Especially, unlike conventional two-terminal synapses, the strain-induced piezo-potential in ZnO could be treated as a virtual gate voltage to

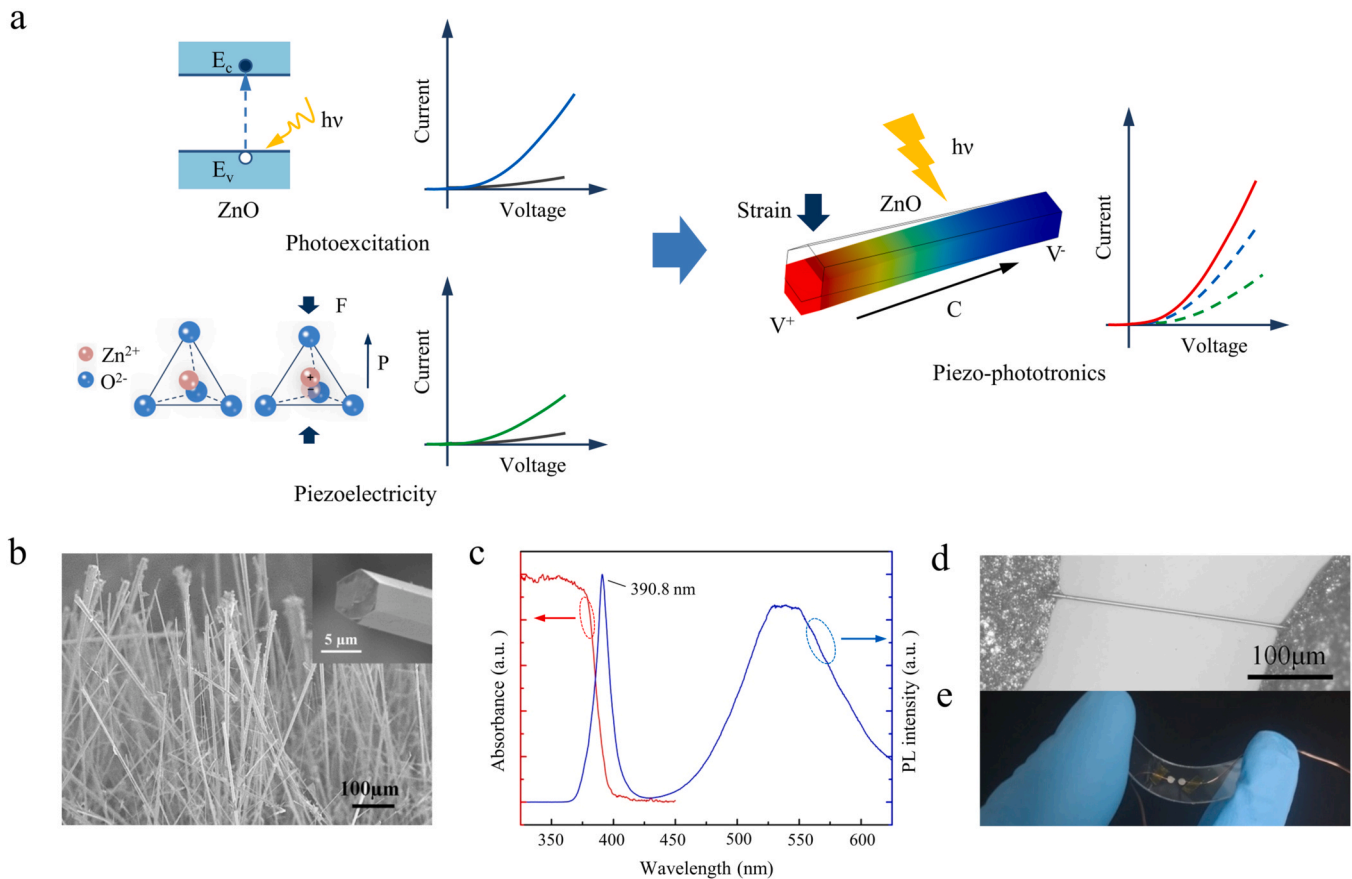


**Fig. 1.** (a) Conception diagram of piezo-phototronic effect for modulating ZnO MNW-based photonic synapse. (b) Scanning electron microscopy (SEM) image of ZnO MNWs; Inset: enlarged SEM image of an individual ZnO MW. (c) The UV-vis absorption and photoluminescence (PL) spectrum of ZnO MNWs. (d,e) Optical microscopy and digital image of a typical synapse device, respectively.

modulate the synaptic plasticity. The UV light pulse at the wavelength of 365 nm is used to train the photonic synapse for the ZnO MNW with a bandgap of 3.28 eV. The conductance of the device is regarded as the synaptic weight.

Fig. 2b shows a response current of the photonic synapse triggered by a light pulse with a wavelength of 365 nm, a light intensity of  $1.66 \text{ mW cm}^{-2}$ , and a width of 1 s. The current reaches its maximum value of about  $0.62 \text{ }\mu\text{A}$  under light pulse, and then decays gradually in dark for the recombination of photo-generated electron-hole pairs caused by oxygen vacancies in ZnO and reaction with chemisorbed oxygen on the ZnO surface [15,35]. This dynamic behavior for the light response that is known as an excitatory postsynaptic current (EPSC) is similar with the behavior in a biological synapse. Fig. 2c depicts the synaptic current triggered by light pulses ( $0.183 \text{ mW cm}^{-2}$ , a width of 1 s) with different interval time for 1 s, 5 s and 10 s, respectively. The current reaches  $0.36 \text{ }\mu\text{A}$  after ten successive pulse trains with an interval time of 1 s (top of Fig. 2c), and  $0.20 \text{ }\mu\text{A}$  after four successive pulse trains with an interval time of 5 s (middle of Fig. 2c), as marked on Fig. 2c. Under the successive short pulse illumination, the electron-hole pair generation is dominating, resulting in the rapid increase of the response current. The shorter the interval time lasts, the more the electrons accumulate. Then, the response current for the condition (a width of 1 s, an interval time of 1 s, and ten times) is higher than the peak value for interval time of 5 s and 10 s. The trace that current reached out to its max value is analogous to a learning process, and meanwhile, the relaxation behavior is just like a forgetting process. The repetitive identical UV light pulse could enhance the current and then delay the relaxation time, result in the transition from STP to LTP. In addition, the STP and LTP corresponding to short-term memory (STM) and long-term

memory (LTM) in the human brain, respectively. It indicates that the emulation of typical transition from STM to LTM could be potentially realized by applying repeatedly UV pulses in human learning activities [35].

The PPF is a common but important phenomenon for short-term synaptic plasticity, in which the post-synaptic response is evoked by the second light pulse following closely behind the first one, as shown in Fig. 2d. The PPF index is defined as a ratio of  $A_2$  to  $A_1$ , where  $A_1$  and  $A_2$  are the values of the first and second post-synaptic current triggered by first and second light pulse, respectively [36,37]. In Fig. 2d, the maximum of PPF index at 1.45 was obtained at the beginning, and the PPF decreases gradually with the increase of the interval time. The decay behavior could fit with a double-exponential function,

$$PPF = 1 + C_1 \exp(-\Delta t/\tau_1) + C_2 \exp(-\Delta t/\tau_2) \quad (1)$$

where  $C_1$  and  $C_2$  are fitting parameters,  $\tau_1$  and  $\tau_2$  are the characteristics decay time constants. The relaxation behavior of PPF is similar to the behavior of biological synapse, indicating that the single ZnO MNW synapse could emulate the function of a biological synapse with a similar double-exponential function [38,39].

The I-V curves of the photonic synapse under different light intensities varying from  $0.003$  to  $1.975 \text{ mW cm}^{-2}$  are displayed in Fig. 3a. It exhibits excellent 365 nm UV response and rectification characteristics at each light intensity. In addition, the photocurrents of the device increase with the light intensity elevating up, because the number of photo-generated electron-hole pairs is proportional to the number of photons absorbed in ZnO. In Fig. 3b, the current is increased by 3 times (from  $0.10 \text{ }\mu\text{A}$  to  $0.30 \text{ }\mu\text{A}$ ) as the compressive strain changed from  $-0.00\%$  to  $-0.32\%$ . It clearly shows the significant enhancements in the

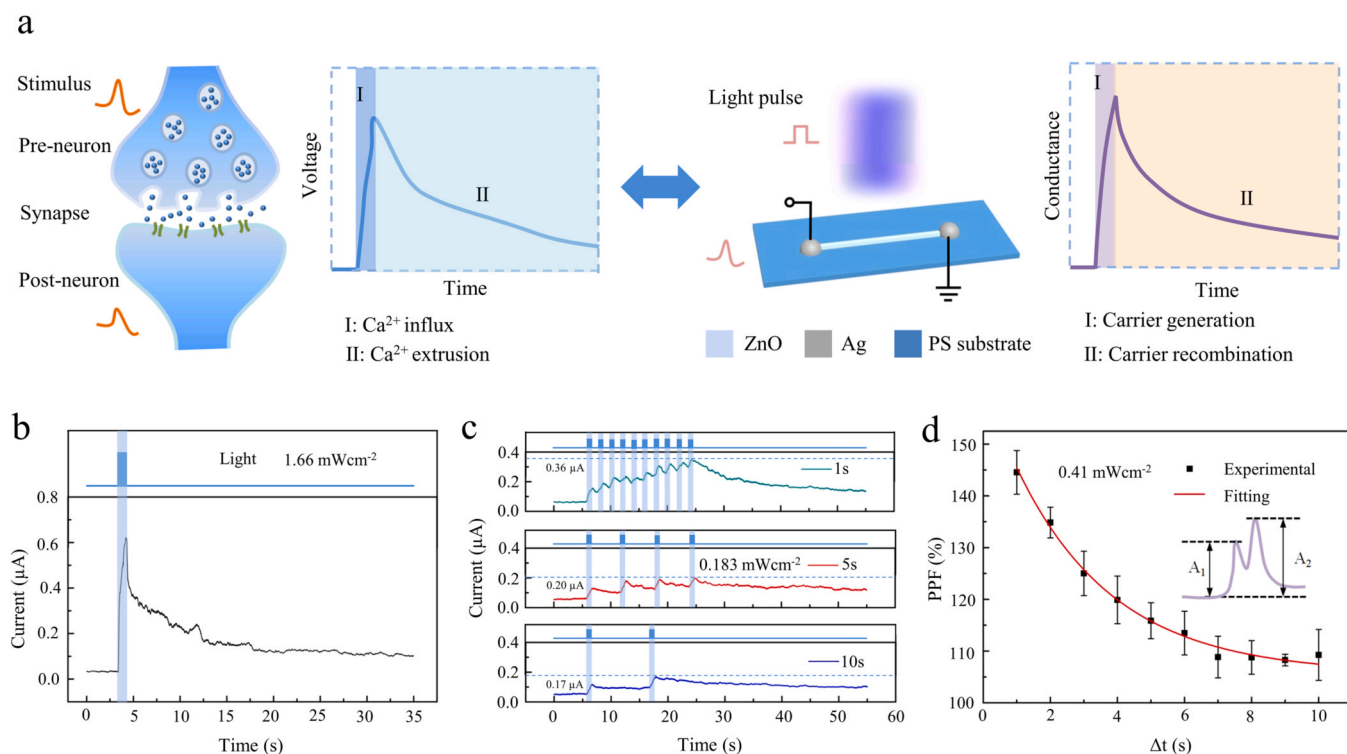


**Fig. 2.** (a) Schematic of biological synapse and  $\text{Ca}^{2+}$  dynamics, and the photonic synapse based on ZnO MNW and its light response. (b) A response current of the synapse triggered by a light pulse with the wavelength of 365 nm, the light intensity of  $1.66 \text{ mW cm}^{-2}$ , and a width of 1 s. (c) The response currents of a synapse triggered by light pulses with a light intensity of  $0.183 \text{ mW cm}^{-2}$ , a width of 1 s, and different interval time for 1 s, 5 s and 10 s, respectively. (d) The PPF emulated by two identical light pulses with a light intensity of  $0.41 \text{ mW cm}^{-2}$ . Inset: schematic of the change in current triggered by two sequential light pulses.

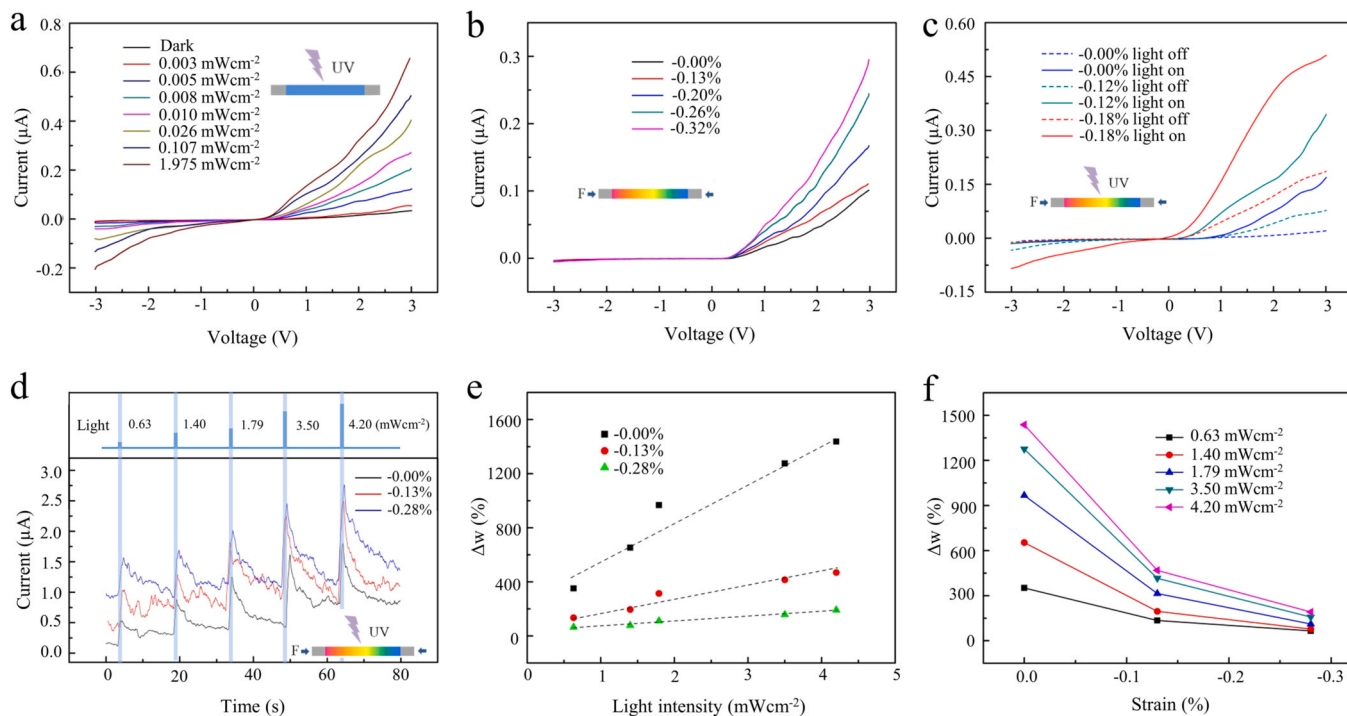


**Fig. 3.** (a) I-V curves of the synapse device under 365 nm UV light with different light intensities. (b) I-V curves of the device with different compressive strains. (c) I-V curves of the device under  $0.468 \text{ mW cm}^{-2}$  light intensity with/without compressive strains. (d) The response currents triggered by different light intensities with different compressive strains. (e) The synaptic weight change varies at different light intensities, with fixed compressive strain in each curve. (f) The synaptic weight change varies at different strains, with fixed light intensity in each curve.



output current of ZnO MNW synapse under compressive strain due to the piezotronic effect. The I-V curves of the device under compressive strains at a 365 nm UV light with a light intensity of  $0.468 \text{ mW cm}^{-2}$  are shown in Fig. 3c. The dashed line and solid line with the same color represent responses in dark and under UV light illumination at the same condition of strain, respectively. It is obvious that photocurrents of the device are significantly improved by applying different compressive strain. The slight fluctuation of the curve may be caused by the property of the interface contact between the ZnO and silver paste [28–30]. Under the UV light ( $0.468 \text{ mW cm}^{-2}$ ), the photocurrents are  $0.17 \mu\text{A}$ ,  $0.34 \mu\text{A}$ , and  $0.51 \mu\text{A}$  with the compressive strain of  $-0.00\%$ ,  $-0.12\%$ , and  $-0.18\%$ , respectively. The current is increased by about 3 times when applying the compressive strain of  $-0.18\%$ . It demonstrates an effective enhancement on the performance of photonic synapse under the piezo-phototronic effect. From Fig. 3a–c, these results clearly indicate that the single ZnO MNW photonic synapse has an excellent piezoelectric property and photoresponse under UV light.

To investigate the piezo-phototronic modulation on the synaptic plasticity of the photonic synapse, the device is studied by synergistically applying UV light pulse trains with different intensities from  $0.63$  to  $4.2 \text{ mW cm}^{-2}$  and strains ranging from  $-0.00\%$  to  $-0.28\%$ , and the corresponding results are demonstrated in Fig. 3d. It clearly shows that the current increases gradually with an increase in light density at the same compressive strain. When the light intensity increases from  $0.63$  to  $4.2 \text{ mW cm}^{-2}$ , the current increases from  $0.53 \mu\text{A}$  to  $1.80 \mu\text{A}$  without strains. Meanwhile, the relaxation time also is prolonged with light intensity boosting up, not returning to its initial state but positioned at a certain higher level. A stronger light pulse would be expected to produce a longer relaxation time for recombination of a large number of carriers. It demonstrates a transition of STP to LTP is caused by a larger light intensity ( $4.2 \text{ mW cm}^{-2}$ ). When compressive strains are applied onto the device, the magnitude of the current and relaxation time improved with the increase of compressive strain under the same light intensity. At a light intensity of  $0.63 \text{ mW cm}^{-2}$ , the current are  $0.53 \mu\text{A}$ ,  $1.04 \mu\text{A}$ , and  $1.57 \mu\text{A}$  for the compressive strains of  $-0.00\%$ ,  $-0.13\%$ , and  $-0.28\%$ , respectively. It could be seen that the transition of STP to LTP could be modulated by introducing external strain, which is a novel result of enhancement in the piezo-phototronic effect [35].

To further illustrate the modulation on the synaptic plasticity by the piezo-phototronic effect, the weight change with respect to different 365 nm UV light intensity and strain conditions are calculated and summarized in Fig. 3e and f, correspondingly. Fig. 3e presents the synaptic weight change under different light intensities, with a fixed compressive strain in each curve, ranging from  $-0.00\%$  to  $-0.28\%$ . At the light intensity of  $4.2 \text{ mW cm}^{-2}$ , the weight change reduces from  $1437.5\%$  to  $191.4\%$  (by almost 7.5 times) as the compressive strain changes from  $-0.00\%$  to  $-0.28\%$ . Fig. 3f shows the synapse weight change under different strains with fixed light intensities in each curve (the light intensities from  $0.63$  to  $4.20 \text{ mW cm}^{-2}$ ). The larger strain

could tune the synapse weight change under different light intensities more substantially. From Fig. 3e and f, it is obvious that the weight change could be regulated and controlled by externally applied compressive strains on the device under the piezo-phototronic effect.

As an important form of synaptic plasticity, LTP is widely believed to underlie learning and memory [40–42]. For a photonic synapse, the relaxation behavior should be controlled for application in neuromorphic computing [15,43]. To control the relaxation behavior, the photonic synapse are investigated by using different compressive strains and applying light pulse trains with a width of 1 s and an interval time of 1 s. The conductance and weight change of the device are shown in Fig. 4a and b, respectively. The conductance is significantly enhanced with the increase of compressive strain, as shown in Fig. 4a. Under a light intensity of  $0.227 \text{ mW cm}^{-2}$ , the conductance reaches  $132.4 \text{ nS}$ ,  $187.7 \text{ nS}$  and  $291.5 \text{ nS}$  for  $-0.00\%$ ,  $-0.15\%$ ,  $-0.22\%$  compressive strain after triggered by ten light pulses, respectively. In Fig. 4b, the synaptic weight change reduces with the increase of compressive strain. The weight change significantly decreases from  $302.4\%$  to  $143.0\%$ , with the increase of compressive strain from  $-0.00\%$  to  $-0.22\%$ . The results confirm that the weight change could be strongly modulated via an applied external strain. The LTP also shows different behavior after applied strains, and the maintained synaptic weight change are larger in  $-0.00\%$  ( $191.8\%$ ) than that of  $-0.22\%$  ( $96.6\%$ ) after 22 s.

$A_n/A_1$  index is defined as the ratio of the peak current amplitudes of light response by first ( $A_1$ ) and  $n$ th light pulses ( $A_n$ ) [15]. The  $A_n/A_1$  index for the LTP under different compressive strains are shown in Fig. 4c. The conductance amplification was  $228.0\%$ ,  $194.6\%$ , and  $174.3\%$  larger than the initial one under  $-0.00\%$ ,  $-0.15\%$ , and  $-0.22\%$  of compressive strain, respectively. The amplification reduced with an increase in compressive strain. These results demonstrates that the compressive strain applied in the device could be used to tune the synaptic functions in the photonic synapse based on a single ZnO MNW for neuromorphic systems.

In the metal-semiconductor-metal (M-S-M) structure, the performance of the device with Schottky contact is mainly determined by the reverse-biased Schottky barrier ( $\Phi_d$ ), and the current density passing through the Schottky barrier ( $J_r$ ) under the applied bias  $V_D$  is given by [44,45]:

$$J_r = \frac{A^* T (\pi E_{00})^{1/2}}{\kappa} \left[ q(V_D - \xi) + \frac{q\phi_b}{\cos h^2(E_{00}/\kappa T)} \right]^{1/2} \times \exp\left(-\frac{q\phi_b}{E_0}\right) \exp\left[qV_D\left(\frac{1}{\kappa T} - \frac{1}{E_0}\right)\right] \quad (2)$$

where  $A^*$  is the Richardson constant of the ZnO NW,  $\xi$  is the distance between Fermi level and the bottom of the conduction band for ZnO wire,  $q$  is the magnitude of electron charge,  $\kappa$  is the Boltzmann constant, and  $T$  is temperature. Then, the two important constants are defined by:

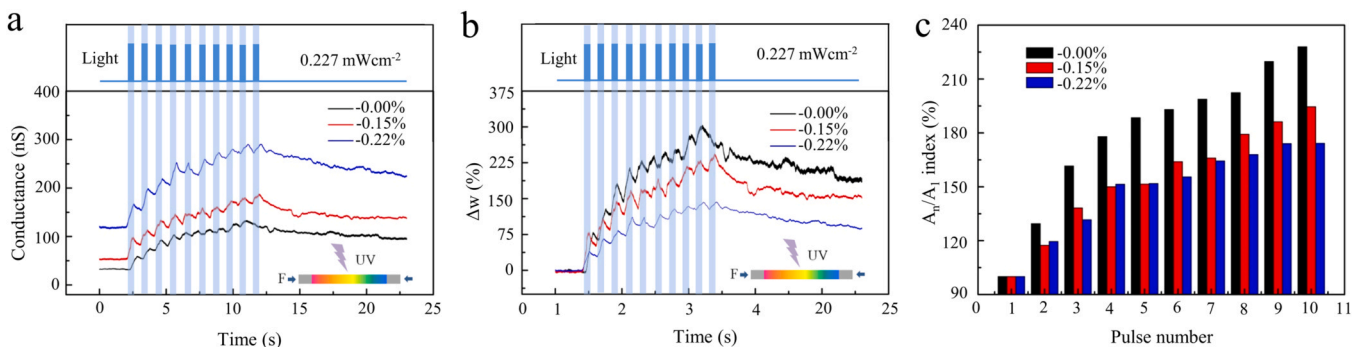


**Fig. 4.** (a) The conductance and weight change of the synapse under different compressive strains by applying ten light pulses with a width of 1 s and an interval time of 1 s. (c)  $A_n/A_1$  index according to the number of light pulses under different compressive strains.

$$E_0 = E_{00} \coth\left(\frac{E_{00}}{\kappa T}\right) \quad (3)$$

$$E_{00} = \frac{\hbar q}{2} \left(\frac{N_d}{m^* \epsilon_s \epsilon_0}\right)^{1/2} \quad (4)$$

where  $N_d$  is the doping density of the ZnO wire,  $m^*$  is the effective mass, and  $\epsilon_s$  and  $\epsilon_0$  are relative permittivity of ZnO NW and absolute permittivity of free space, respectively. From Eq. (2), the current density  $J$ , has an exponential relationship with the reverse-biased Schottky barrier  $\Phi_d$ , indicating that a tiny change of  $\Phi_d$  could cause a relatively large change in current. Based on the M-S-M structure, a linear region is expected for the I-V curve at large bias, so the resistance of the ZnO NW could be determined from the linear region by:

$$R_{ZnO} \approx \frac{dV}{dI}\bigg|_{\text{large bias}} \quad (5)$$

For in-depth understanding of the piezo-phototronic modulation of the photonic synapse, an equivalent circuit model for the M-S-M structure (inset of Fig. 5a) is built, and the fitting of the I-V curves of the devices in Fig. 3c is carried out by utilizing a GUI program PKUMSM developed by Peng et al. [43]. As shown in Fig. 5a, the fitting result of the I-V curve at  $-0.18\%$  of compressive strain in dark conditions is plotted as a red line and agrees well with the experimental data in blue dots. Based on the equivalent circuit model, the  $\Phi_d$  and  $R_{ZnO}$  are extracted from Fig. 3c as presented in Fig. 5b and c. It is obvious that both of the  $\Phi_d$  in the condition of light on or light off decrease obviously as introducing more compressive strains on the devices, but the change of  $\Phi_d$  is small before light on or off. The change of  $\Phi_d$  effectively dominates the charge carriers transport process across the local interface. Thus, the enhancement of photocurrent is largely due to the strain-induced piezoelectric potential. According to Fig. 5c, the fluctuation trend for the resistances of ZnO MNW  $R_{ZnO}$  is similar to the change of  $\Phi_d$  under compressive strains, but the change is much smaller. However, the change of the resistances decreases obviously before and after UV illumination. From Fig. 5b and c, the decrease of  $\Phi_d$  and  $R_{ZnO}$  might be accounted for the increase of the current.

Band diagrams of the photonic synapse are carefully analyzed and studied to illustrate the physical mechanism through the observed synaptic behaviors and modulation by the piezo-phototronic effect based on a single ZnO MNW, as shown in Fig. 6. A Schottky contact is formed at local metal-semiconductor (M-S) contact (reversely biased drain electrode) in vacuum as shown in Fig. 6a. In Fig. 6b, the  $O_2$  molecules are adsorbed on the ZnO surface and a depletion layer is formed in the air, and the oxygen vacancies in ZnO trap the electrons, therefore this process reduces the number of free electrons inside the pristine ZnO MNW, leading to a lower conductivity and output current [46–48].

As shown in Fig. 6c, under UV illumination, the photo-generated electron-hole pairs could react with chemisorbed oxygen on the surface, thin the depletion layer and increase electrons, resulting in an

upward current. Once UV light turns off, the oxygen absorption takes place on the surface of ZnO again. Moreover, the oxygen vacancies in ZnO could trap the electrons, or act as the recombination centers to accelerate the recombination process and reduce carrier migration rate. These processes would consume the free electrons, leading to the current decaying gradually [29,49]. In Fig. 6d, when the compressive strain is applied along the c-axis of ZnO MNW under UV illumination, the positive piezoelectric polarization charges are created at the local M-S contact and modified the band structure at the M-S interface, effectively reducing the  $\Phi_d$ . The piezo-phototronic effect could enhance the separation efficiency of the photo-generated electron-hole pairs and decrease the possibility of recombination, then reduced the depletion layer and increased carrier concentration [18,20,50]. The result leads to the enhancements on output current as well as the general performances of the device.

Finally, in order to further perform the learning capability of photonic synapse, an artificial neural network (ANN) based on single-layer perceptron (SLP) is designed and simulated to demonstrate the image recognition accuracy for the Modified National Institute of Standards and Technology (MNIST) database, as shown in Fig. S1. In Fig. S2, the synaptic characteristics such as the conductance margin  $G_{\max}/G_{\min}$ , nonlinearity (NL) value can be extracted for simulation. As shown in Fig. S3, the recognition accuracy with different strain conditions after supervised learning can be improved by the piezo-phototronic effect.

#### 4. Conclusions

In summary, based on an M-S-M structure, we have fabricated transparent and flexible photonic synapse devices using a single ZnO MNW. The synaptic functions such as PPF, STP, and LTP could be obtained by applying the UV light pulse stimuli. Under compressive strains, the piezo-phototronic effect has been introduced to modulate the photon-generated carriers transport process across the M-S contact and tuned the synaptic plasticity behavior. The weight change reduces from 1437.5% to 191.4% with an increase of compressive strain. The relaxation characteristics of the synapse could also be modulated by the piezo-phototronic effect through controlling effectively the transport of photo-generated carriers in ZnO. Furthermore, artificial neural networks are simulated to demonstrate the image recognition accuracy can be improved by the piezo-phototronic effect. This work provides an effective approach to designing and controlling the photonic synapse based on piezoelectric semiconductors in the area of smart systems, artificial intelligence, and neuromorphic computing.

#### CRediT authorship contribution statement

**Guofeng Hu:** Writing - original draft, Investigation, Formal analysis, Methodology, Simulation. **Hua An:** Formal analysis, Methodology, Writing - review & editing. **Jianguo Xi:** Investigation, Methodology,

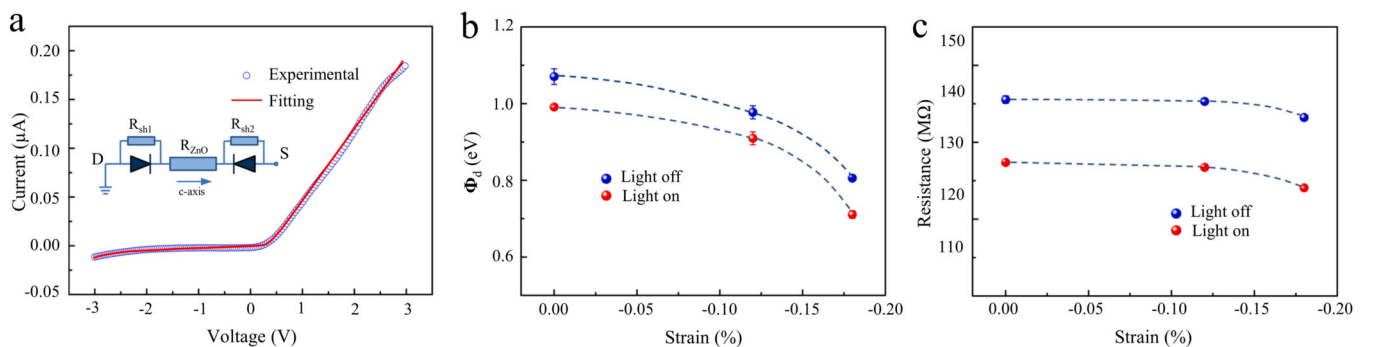


**Fig. 5.** (a) The equivalent circuit model and quantitative fitting result of an photonic synapse based on ZnO MNW. (b) The fitting results of the Schottky barrier changes with strains for light on and light off. (c) The fitting results of the resistance of the ZnO MNW changes with strains for light on and light off.

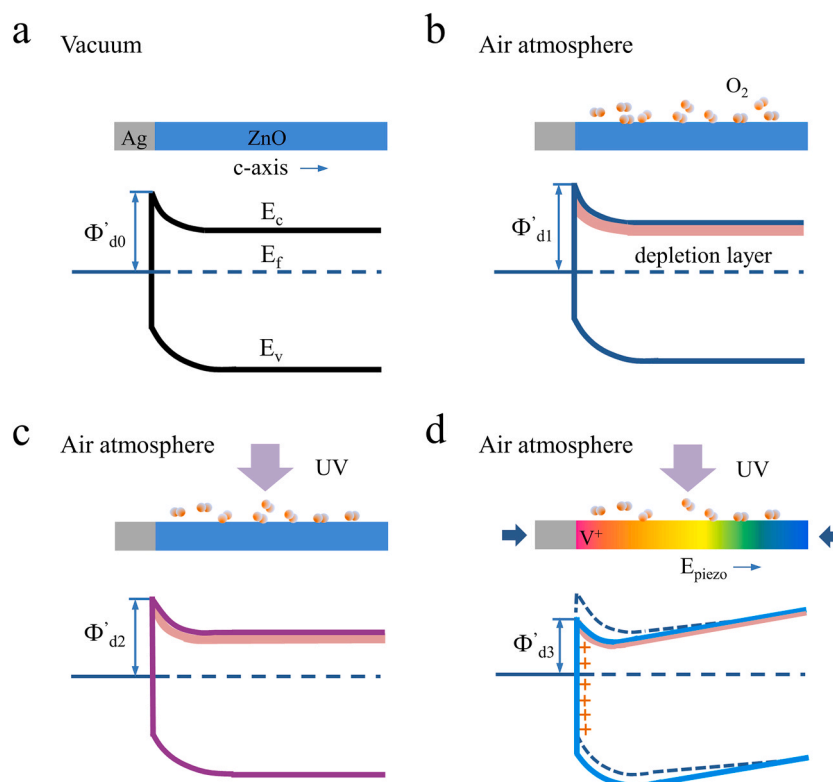


**Fig. 6.** The physical mechanism for the photonic synapse modulated by the piezo-phototronic effect. Schematic energy band diagrams of ZnO MNW in (a) vacuum; (b) air atmosphere; (c) air atmosphere with UV illumination; (d) air atmosphere under compressive strains with UV illumination.

Software. **Junfeng Lu:** Investigation, Methodology, Software. **Qilin Hua:** Resources, Validation, Supervision. **Zhengchun Peng:** Writing - review & editing, Project administration, Supervision, Funding acquisition.

#### Declaration of Competing Interest

The authors declare that they have no known competing financial interests or personal relationships that could have appeared to influence the work reported in this paper.

#### Acknowledgements

This work was financially supported by the Science and Technology Innovation Commission of Shenzhen, China (JCYJ20200109114237902, KQTD20170810105439418, JCYJ20170818091233245), the National Natural Science Foundation of China, China (22005198, 61904012), the Natural Science Foundation of Beijing Municipality, China (4204114), the China Postdoctoral Science Foundation Funded Project, China (Grant No. 2017M620709).

#### Appendix A. Supporting information

Supplementary data associated with this article can be found in the online version at [doi:10.1016/j.nanoen.2021.106282](https://doi.org/10.1016/j.nanoen.2021.106282).

#### References

- M. Prezioso, F.M. -Bayat, B.D. Hoskins, G.C. Adam, K.K. Likharev, D.B. Strukov, Training and operation of an integrated neuromorphic network based on metal-oxide memristors, *Nature* 521 (2015) 61–64.
- Y. Kim, A. Chortos, W. Xu, Y. Liu, J.Y. Oh, D. Son, J. Kang, A.M. Foudeh, C. Zhu, Y. Lee, S. Niu, J. Liu, R. Pfattner, Z. Bao, T.-W. Lee, A bioinspired flexible organic artificial afferent nerve, *Science* 360 (2018) 998–1003.
- Z. Cheng, C. Ríos, W.H.P. Pernice, C.D. Wright, H. Bhaskaran, On-chip photonic synapse, *Sci. Adv.* 3 (2017), e1700160.
- Q. Hua, H. Wu, B. Gao, Q. Zhang, W. Wu, Y. Li, X. Wang, W. Hu, H. Qian, Low-voltage oscillatory neurons for memristor-based neuromorphic systems, *Glob. Chall.* 3 (2019), 1900015.
- Q. Hua, H. Wu, B. Gao, M. Zhao, Y. Li, X. Li, X. Hou, M. Chang, P. Zhou, H. Qian, A threshold switching selector based on highly ordered Ag nanodots for X-Point memory applications, *Adv. Sci.* 6 (2019), 1900024.
- Q. Hua, X. Cui, H. Liu, C. Pan, W. Hu, Z.L. Wang, Piezotronic synapse based on a single GaN microwire for artificial sensory systems, *Nano Lett.* 20 (2020) 3761–3768.
- Y. Wang, Z. Lv, J. Chen, Z. Wang, Y. Zhou, L. Zhou, X. Chen, S.-T. Han, Photonic synapses based on inorganic perovskite quantum dots for neuromorphic computing, *Adv. Mater.* 30 (2018), 1802883.
- G. Milano, M. Luebben, Z. Ma, R. Dunin-Borkowski, L. Boarino, C.F. Pirri, R. Waser, C. Ricciardi, I. Valov, Self-limited single nanowire systems combining all-in-one memristive and neuromorphic functionalities, *Nat. Commun.* 9 (2018) 5151.
- M. Kumar, S. Abbas, J. Kim, All-oxide-based highly transparent photonic synapse for neuromorphic computing, *ACS Appl. Mater. Interfaces* 10 (2018) 34370–34376.
- A.F. Benner, M. Ignatowski, J.A. Kash, D.M. Kuchta, M.B. Ritter, Exploitation of optical interconnects in future server architectures, *IBM J. Res. Dev.* 49 (2005) 755–775.
- D.-C. Hu, R. Yang, L. Jiang, X. Guo, Memristive synapses with photoelectric plasticity realized in ZnO<sub>1-x</sub>/AlO<sub>y</sub> heterojunction, *ACS Appl. Mater. Interfaces* 10 (2018) 6463–6470.
- H.K. Li, T.P. Chen, P. Liu, S.G. Hu, Y. Liu, Q. Zhang, P.S. Lee, A light-stimulated synaptic transistor with synaptic plasticity and memory functions based on InGaZnO<sub>x</sub>-Al<sub>2</sub>O<sub>3</sub> thin film structure, *J. Appl. Phys.* 119 (2016), 244505.
- Q. Wu, J. Wang, J. Cao, C. Lu, G. Yang, X. Shi, X. Chuai, Y. Gong, Y. Su, Y. Zhao, N. Lu, D. Geng, H. Wang, L. Li, M. Liu, Photoelectric plasticity in oxide thin film transistors with tunable synaptic functions, *Adv. Electron. Mater.* 4 (2018), 1800556.
- S. Jeon, S.-E. Ahn, I. Song, C.J. Kim, U.I. Chung, E. Lee, I. Yoo, A. Nathan, S. Lee, J. Robertson, Gated three-terminal device architecture to eliminate persistent photoconductivity in oxide semiconductor photosensor arrays, *Nature Mater.* 11 (2012) 301–305.
- M.-K. Kim, J.-S. Lee, Synergistic improvement of long-term plasticity in photonic synapses using ferroelectric polarization in hafnia-based oxide-semiconductor transistors, *Adv. Mater.* 32 (2020), 1907826.
- M. Kumar, R. Singh, H. Kang, S. Kim, H. Seo, An artificial piezotronic synapse for tactile perception, *Nano Energy* 73 (2020), 104756.
- Y. Zhang, Y. Liu, Z.L. Wang, Fundamental theory of piezotronics, *Adv. Mater.* 23 (2011) 3004–3013.
- Z.L. Wang, Piezopotential gated nanowire devices: piezotronics and piezophototronics, *Nano Today* 5 (2010) 540–552.

- [19] W. Wu, C. Pan, Y. Zhang, X. Wen, Z.L. Wang, Piezotronics and piezo-phototronics—from single nanodevices to array of devices and then to integrated functional system, *Nano Today* 8 (2013) 619–642.
- [20] Z.L. Wang, Piezotronic and piezophototronic effects, *J. Phys. Chem. Lett.* 1 (2010) 1388–1393.
- [21] Q. Hua, J. Sun, H. Liu, X. Cui, K. Ji, W. Guo, C. Pan, W. Hu, Z.L. Wang, Flexible GaN microwire-based piezotronic sensory memory device, *Nano Energy* 78 (2020), 105312.
- [22] X. Han, W. Du, R. Yu, C. Pan, Z.L. Wang, Piezo-phototronic enhanced UV sensing based on a nanowire photodetector array, *Adv. Mater.* 27 (2015) 7963–7969.
- [23] Q. Xu, Z. Yang, D. Peng, J. Xi, P. Lin, Y. Cheng, K. Liu, C. Pan,  $WS_2/CsPbBr_3$  van der Waals heterostructure planar photodetectors with ultrahigh on/off ratio and piezo-phototronic effect-induced strain-gated characteristics, *Nano Energy* 65 (2019), 104001.
- [24] G. Hu, W. Guo, R. Yu, X. Yang, R. Zhou, C. Pan, Z.L. Wang, Enhanced performances of flexible ZnO/perovskite solar cells by piezo-phototronic effect, *Nano Energy* 23 (2016) 27–33.
- [25] J. Sun, Q. Hua, R. Zhou, D. Li, W. Guo, X. Li, G. Hu, C. Shan, Q. Meng, L. Dong, C. Pan, Z.L. Wang, Piezo-phototronic effect enhanced efficient flexible perovskite solar cells, *ACS Nano* 13 (2019) 4507–4513.
- [26] C. Pan, L. Dong, G. Zhu, S. Niu, R. Yu, Q. Yang, Y. Liu, Z.L. Wang, High-resolution electroluminescent imaging of pressure distribution using a piezoelectric nanowire LED array, *Nature Photon.* 7 (2013) 752–758.
- [27] T. Liu, D. Li, H. Hu, X. Huang, Z. Zhao, W. Sha, C. Jiang, C. Du, M. Liu, X. Pu, B. Ma, W. Hu, Z.L. Wang, Piezo-phototronic effect in InGaN/GaN semi-floating micro-disk LED arrays, *Nano Energy* 67 (2020), 104218.
- [28] W. Wu, Z.L. Wang, Piezotronics and piezo-phototronics for adaptive electronics and optoelectronics, *Nat. Rev. Mater.* 1 (2016) 16031.
- [29] C. Pan, J. Zhai, Z.L. Wang, Piezotronics and piezo-phototronics of third generation semiconductor nanowires, *Chem. Rev.* 119 (2019) 9303–9359.
- [30] R. Zhou, G. Hu, R. Yu, C. Pan, Z.L. Wang, Piezotronic effect enhanced detection of flammable/toxic gases by ZnO micro/nanowire sensors, *Nano Energy* 12 (2015) 588–596.
- [31] M. Chen, B. Zhao, G. Hu, X. Fang, H. Wang, L. Wang, J. Luo, X. Han, X. Wang, C. Pan, Z.L. Wang, Piezo-phototronic effect modulated deep UV photodetector based on ZnO-Ga<sub>2</sub>O<sub>3</sub> heterojunction microwire, *Adv. Funct. Mater.* 28 (2018), 1706379.
- [32] C. Pan, J. Zhu, The syntheses, properties and applications of Si, ZnO, metal, and heterojunction nanowires, *J. Mater. Chem.* 19 (2009) 869–884.
- [33] G. Zhu, Y. Zhou, S. Wang, R. Yang, Y. Ding, X. Wang, Y. Bando, Z.L. Wang, Synthesis of vertically aligned ultra-long ZnO nanowires on heterogeneous substrates with catalyst at the root, *Nanotechnology* 23 (2012), 055604.
- [34] A. Janotti, C.G. Van de Walle, Oxygen vacancies in ZnO, *Appl. Phys. Lett.* 87 (2005), 122102.
- [35] M. Kumar, J. Kim, C.-P. Wong, Transparent and flexible photonic artificial synapse with piezo-phototronic modulator: versatile memory capability and higher order learning algorithm, *Nano Energy* 63 (2019), 103843.
- [36] L. Yin, W. Huang, R. Xiao, W. Peng, Y. Zhu, Y. Zhang, X. Pi, D. Yang, Optically stimulated synaptic devices based on the hybrid structure of silicon nanomembrane and perovskite, *Nano Lett.* 20 (2020) 3378–3387.
- [37] L. Yang, M. Singh, S.-W. Shen, K.-Y. Chih, S.-W. Liu, C.-I. Wu, C.-W. Chu, H.-W. Lin, Transparent and flexible inorganic perovskite photonic artificial synapses with dual-mode operation, *Adv. Funct. Mater.* 31 (2021), 2008259.
- [38] R.S. Zucker, W.G. Regehr, Short-term synaptic plasticity, *Annu. Rev. Physiol.* 64 (2002) 355–405.
- [39] P.A. Salin, M. Scanziani, R.C. Malenka, R. Nicoll, Distinct short-term plasticity at two excitatory synapses in the hippocampus, *Proc. Natl. Acad. Sci. USA* 93 (1996) 13304–13309.
- [40] T.V.P. Bliss, G.L. Collingridge, A synaptic model of memory: long-term potentiation in the hippocampus, *Nature* 361 (1993) 31–39.
- [41] T. Ohno, T. Hasegawa, T. Tsuruoka, K. Terabe, J.K. Gimzewski, M. Aono, Short-term plasticity and long-term potentiation mimicked in single inorganic synapses, *Nature Mater.* 10 (2011) 591–595.
- [42] S. Yu, Neuro-inspired computing with emerging nonvolatile memory, *Proc. IEEE* 106 (2018) 260–285.
- [43] Z. Wang, S. Joshi, S.E. Savel'ev, H. Jiang, R. Midya, P. Lin, M. Hu, N. Ge, J. P. Strachan, Z. Li, Q. Wu, M. Barnell, G.-L. Li, H.L. Xin, R.S. Williams, Q. Xia, J. J. Yang, Memristors with diffusive dynamics as synaptic emulators for neuromorphic computing, *Nature Mater.* 16 (2017) 101–108.
- [44] Y. Liu, Z.Y. Zhang, Y.F. Hu, C.H. Jin, L.M. Peng, Quantitative fitting of nonlinear current-voltage curves and parameter retrieval of semiconducting nanowire, nanotube and nanoribbon devices, *J. Nanosci. Nanotechnol.* 8 (2008) 252–258.
- [45] R. Yu, L. Dong, C. Pan, S. Niu, H. Liu, W. Liu, S. Chua, D. Chi, Z.L. Wang, Piezotronic effect on the transport properties of GaN nanobelts for active flexible electronics, *Adv. Mater.* 24 (2012) 3532–3537.
- [46] Z. Fan, P.C. Chang, J.G. Lu, E.C. Walter, R.M. Penner, C.H. Lin, H.P. Lee, Photoluminescence and polarized photodetection of single ZnO nanowires, *Appl. Phys. Lett.* 85 (2004) 6128–6130.
- [47] H.-S. Kim, S.H. Jeon, J.S. Park, T.S. Kim, K. Kim, Anion control as a strategy to achieve high-mobility and high-stability oxide thin-film transistors, *Sci. Rep.* 3 (2013) 1459.

- [48] M. Kumar, T. Basu, T. Som, Ultra-violet absorption induced modifications in bulk and nanoscale electrical transport properties of Al-doped ZnO thin films, *J. Appl. Phys.* 118 (2015), 055102.
- [49] M. Law, H. Kind, B. Messer, F. Kim, P. Yang, Photochemical sensing of NO<sub>2</sub> with SnO<sub>2</sub> nanoribbon nanosensors at room temperature, *Angew. Chem. Int. Ed.* 41 (2002) 2405–2408.
- [50] L. Ying, Q. Yang, Y. Zhang, Z. Yang, Z.L. Wang, Nanowire piezo-phototronic photodetector: theory and experimental design, *Adv. Mater.* 15 (2012) 1410–1417.



**Dr. Guofeng Hu** received his Ph.D. from Beijing Institute of Nanoenergy and Nanosystems, CAS under the supervision of Prof. Caofeng Pan in 2015. Currently, he is a post-doctoral researcher at Shenzhen University. His research is mainly focused on photoelectric devices and electronic applications of piezotronics and piezophototronics based on low dimensional materials.



**Dr. Hua An** received her Ph.D. from University of Tokyo in Mechanical Engineering in 2017. She is now an associate researcher in Shenzhen University. Her research interests focus on the controlled synthesis of functional nanomaterials and their applications in photoelectronic devices and flexible devices.



**Dr. Jianguo Xi** received his Ph.D. from China University of Geosciences in 2015. He then joined Auburn University as a postdoctoral fellow. Since 2019, he is a joint postdoctoral fellow of Dr. Wenjie Mai's group at Jinan University and Dr. Canfeng Pan's group at Beijing Institute of Nanoenergy and Nanosystem. His main research interests focus on 2D material heterostructures and application.



**Dr. Junfeng Lu** received his Ph.D. degree from Southeast University, China in 2017. He then joined the research group of Professor Zhong Lin Wang at Beijing Institute of Nanoenergy and Nanosystems as a postdoctoral fellow. He is currently an associate professor at Nanjing University of Aeronautics and Astronautics. His main research interests focus on laser regulated optoelectronic devices.





**Dr. Qilin Hua** received his Ph.D. degree in microelectronics from University of Chinese Academy of Sciences in 2016. He then joined Tsinghua University, China. He is currently an associate professor at Beijing Institute of Nanoenergy and Nanosystems, Chinese Academy of Science. His research interests include flexible/stretchable electronics, low-dimensional materials, GaN-based devices, memristors, and neuromorphic systems.



**Dr. Zhengchun Peng** received his Ph.D. degree in MEMS from the Georgia Institute of Technology. He then joined Intel as a senior R&D engineer. He is currently a distinguished professor at Shenzhen University since 2015. His main research interests focus on flexible and stretchable electronics, skin-integrated medical electronics, robotic tactile intelligence, MEMS, and microfluidics.